Hindawi
Mathematical Problems in Engineering
Volume 2019, Article ID 2543584, 17 pages
https://doi.org/10.1155/2019/2543584

Research Article

Evaluation of Ground Surface Pregrouting in a Mountain Tunnel Based on FAHP

Changan Zhu, Runfang Sun, Hua Xu, Yiwei Liu, and Zhuang Chen

Key Laboratory of Transportation Tunnel Engineering, Ministry of Education, School of Civil Engineering, Southwest Jiaotong University, Chengdu 610031, Sichuan, China

Correspondence should be addressed to Hua Xu; xuhua@home.swjtu.edu.cn

Received 19 January 2019; Revised 6 June 2019; Accepted 24 June 2019; Published 3 September 2019

Academic Editor: Jan Vorel

The quality of ground surface pregrouting (GSPG) is commonly qualitatively evaluated using single factor; however, the quality evaluation involves numerous facets, and a quantitative evaluation is rare. The aim of this study was to quantitatively evaluate the quality of a GSPG based on three aspects. The fuzzy analytic hierarchy process (FAHP) was adopted to obtain the final score and quality classification of the GSPG. Based on three aspects, namely, integrity, continuity, and sturdiness, a series of field tests was also conducted, qualitatively evaluating the quality of the GSPG preliminary, to obtain the required test data and verify the FAHP results. The results of the FAHP showed that the quality of the GSPG was 86.42, which could be classified as "Good", whereas the field tests exhibited that the GSPG was effective, thereby verifying that the FAHP was reliable. In addition, the proposed method provided a detailed comprehension of the quality evaluation of GSPG and a frame of reference for analogous engineering.

1. Introduction

Ground surface pregrouting (GSPG) is a technique in which a slurry containing several types of materials, such as cement, mortar, and some chemical polymers, is pumped into boreholes to improve the quality of rock mass and prevent water leakage [1]. Different from general in-tunnel grouting, GSPG is performed on the ground surface before construction, and it is generally utilized in shallow-buried sections as well as portal sections in mountain tunnels [2].

The objective of GSPG is twofold: to improve the quality of the rock mass and prevent tunnel collapse during construction [3–5] and to reduce the permeability rate of the rock mass from ground surface to tunnel bottom and prevent the inrush of the surface water and groundwater [3, 6, 7]. Moreover, GSPG can also reduce the loss of surface water and groundwater caused by karst fissures, which affects the domestic water consumption near shallow-buried sections during tunnel excavation [2, 8].

Generally, the targets of GSPG are the important parts of mountain tunnels, such as portal sections and shallow-buried sections. A poor quality of grouting may lead to geological disasters, such as collapse and water inrush. Hence, the quality evaluation of grouting is vital. This tends to be difficult owing to the complex geological conditions. Typically, the quality is evaluated indirectly using various tests. At present, the water pressure test is a common method [9–12]. Other field tests such as ultrasonic tests have been commonly applied to the quality evaluation of grouting [13]. Moreover, numerous new methods have been employed for evaluation. Xu et al. [14] used self-developed pressure-grouting devices to estimate the strength growth of post- to pregrouting broken rock. Li et al. [15] proposed an HHT (Hilbert–Huang transform)-based method to detect the grouting quality in concrete structures. Wang et al. [4] utilized an analytical solution to predict the ground displacement caused by grouting. However, these studies are based on single factor influencing the grouting quality, which may not be used for quantitative evaluation. Furthermore, studies using multifacet factors for the quality evaluation of GSPG are rare, not in the least for mountain tunnels. More significantly, field tests can be utilized for only qualitatively evaluating the quality. Thus, the quality classification of grouting cannot be achieved by such tests.

Therefore, for multifactor evaluation, a quantitative method is required. The FAHP (fuzzy analytic hierarchy

process), a mathematical method based on fuzzy theory, is used for the quantitative evaluation of an objective [16–19]. Fan et al. [20] proposed a hybrid fuzzy quantitative evaluation method to assess the curtain grouting efficiency of a dam foundation by considering the permeability rate of the grout curtain. Zhang et al. [21] determined the curtain grouting form, hierarchical structure of the layers of the overall target, tool, attribute, and program by the AHP. However, the FAHP is mainly applied to the curtain grouting of dams, and its applications in the GSPG in mountain tunnels are uncommon.

In this study, we have presented three facets: integrity, continuity, and sturdiness, to quantitatively evaluate the quality of a GSPG, using the FAHP. First, a series of field tests regarding the GSPG was performed in the Tongluoshan tunnel of southwest China, and five indices were tested. Then we qualitatively evaluated the quality of the GSPG. Finally, the FAHP was applied to quantitatively evaluate the quality using the five-test data, and the quality classification of the GSPG as well as the final score was obtained.

2. Fuzzy Analytic Hierarchy Process (FAHP)

2.1. Analytic Hierarchy Process (AHP). The analytic hierarchy process (AHP), a powerful and flexible multicriteria decision-making tool for complex problems where both qualitative and quantitative aspects need to be considered, was proposed by Saaty [16, 17]. The AHP not only assists in making the best decision and synthesizing the results but also provides an explicit rationale for the choices made. The AHP encompasses three steps: (a) establishing the AHP model, a hierarchical structure like a "family tree", (b) devising the judgment matrices, and (c) determining the weight matrix.

(a) Establishing the AHP Model. There are three layers in an AHP model: target layer, criterion layer, and index layer. First, the researchers are required to identify the problem, or target of the study in the target layer. Second, the various factors influencing the target are analyzed and then classified in the criterion layer. Finally, the indices are determined for each criterion. The AHP model is shown in Figure 1. As shown in Figure 1, on the target layer, the target set $\mathbf{Z}$ is expressed as in (1)

$$\mathbf{Z} = \{Z\} \tag{1}$$

where $\mathbf{Z}$ is the target set. On the criterion layer, criterion set $\mathbf{U}$ is as expressed in (2)

$$\mathbf{U} = \{U_1, U_2, \cdots, U_n\} \quad (n = 1, 2, 3, \cdots) \tag{2}$$

where $U_1, U_2, \cdots, U_n$ are the criteria influencing the target, Z. Moreover, on the index layer, the index set $\mathbf{P}$ is expressed as given in (3)

$$\mathbf{P} = \{P_{11}, P_{12}, \cdots, P_{1n}, P_{21}, P_{22}, \cdots, P_{2n}, \cdots, P_{n1}, P_{n2}, \cdots, P_{nn}\} \quad (n = 1, 2, 3, \cdots) \tag{3}$$

where P_{1n}, P_{2n}, and P_{nn} denote the indices concerning the criteria.

(b) Devising the Judgment Matrices. Judgment Matrices $\mathbf{A}_Z$ and $\mathbf{A}_{U_n}$ $(n = 1, 2, 3 \cdots)$ were formed using (4) and (5) via a simple pairwise comparisons of all the factors in the criterion layer and index layer.

$$\mathbf{A}_Z = \begin{bmatrix} 1 & a_{12} & \cdots & a_{1j} \\ \frac{1}{a_{12}} & 1 & \cdots & a_{2j} \\ \vdots & \vdots & 1 & \vdots \\ & & & a_{ij} \\ \frac{1}{a_{1j}} & \frac{1}{a_{2j}} & \cdots \frac{1}{a_{ij}} & 1 \end{bmatrix} \tag{4}$$

$$\mathbf{A}_{U_n} = \begin{bmatrix} 1 & b_{12} & \cdots & b_{1j} \\ \frac{1}{b_{12}} & 1 & \cdots & b_{2j} \\ \vdots & \vdots & 1 & \vdots \\ & & & b_{ij} \\ \frac{1}{b_{1j}} & \frac{1}{b_{2j}} & \cdots \frac{1}{b_{ij}} & 1 \end{bmatrix} \tag{5}$$

where a_{ij} and b_{ij} $(i, j = 1, 2, 3 \cdots)$ are the numbers whose values are listed in Table 1 according to the nine-scaling method [16]. For example, the target layer includes U_1, U_2,. . .,U_n, and then element a_{12} is obtained by comparing the importance of U_1 and U_2. If U_1 is slightly more important than U_2, then the value of a_{12} is "3." Similarly, in the criterion layer, the lower layer of factor U_n includes P_{n1}, P_{n2},. . .,P_{nn}, and element b_{12} is obtained by comparing the importance of P_{n1} and P_{n2}. If P_{n1} is more important than P_{n2}, then the value of b_{12} is "5."

(c) Determining the Weight Matrix. Following the establishment of the judgment matrices, the normalized eigenvectors of $\mathbf{A}_Z$ and $\mathbf{A}_{U_n}$ $(n = 1, 2, 3 \cdots)$ are expressed as given in (6) and (7).

$$\mathbf{e}_Z = [a_1 \;\; a_2 \;\; \cdots \;\; a_n] \tag{6}$$

$$\mathbf{e}_{U_n} = [b_{n1} \;\; b_{n2} \;\; \cdots \;\; b_{nn}] \tag{7}$$

where $\mathbf{e}_Z$ and $\mathbf{e}_{U_n}$ are the normalized eigenvectors obtained by solving matrix equations, which can be conducted with MATLAB programming. a_n and b_{nn} $(n = 1, 2, 3 \cdots)$ are specific numbers. Thus, the weight matrix is calculated using (8).

$$\mathbf{W} = [a_1 b_{11} \;\; a_1 b_{12} \;\; \cdots \;\; a_1 b_{1n}; a_2 b_{21} \;\; a_2 b_{22} \;\; \cdots \;\; a_2 b_{2n}; \cdots; a_n b_{n1} \;\; a_n b_{n2} \;\; \cdots \;\; a_n b_{nm}] \tag{8}$$

Table 1: Nine-scaling method [16, 22].

Values	Equal importance with regard to the two indices
1	The two indices are equally important
3	The former is slightly more important than the latter
5	The former is more important than the latter
7	The former is much more important than the latter
9	The former is considerably more important than the latter
2,4,6,8	Intermediate values are used to reflect fuzzy inputs
Reciprocal	The dominance of the second alternative is reflected compared with the first, $a_{ji} = 1/a_{ij}$

Note: Table 1 is reproduced from Xu et al. (2019) [22].

where $\mathbf{W}$ is the weight matrix and a_n, b_{nm} $(n = 1, 2, 3\cdots)$ are elements from the normalized eigenvectors.

2.2. Fuzzy Method. The fuzzy method, which is based on the theory of fuzzy mathematics, was developed by Zadeh [18]. It has four steps: (a) establishing the evaluation set of the target, (b) establishing the evaluation set of each index, (c) calculating the membership of each index, and (d) evaluating the target. The procedure of fuzzy method is as follows.

(a) Establishing the Evaluation Set of the Target. For an evaluation target of a project, all of its possible results can be incorporated in a set $\mathbf{I}$ (see (9)), and each element in set $\mathbf{I}$ can be specified in a range (Table 2).

$$\mathbf{I} = \begin{bmatrix} I_1 & I_2 & \cdots & I_n \end{bmatrix} \tag{9}$$

where I_n $(n = 1, 2, 3\cdots)$ denotes the evaluation results of the target. In Table 2, i_n $(n = 1, 2, 3\cdots)$ represents the description of the evaluation results (e.g., i_1 is excellent, grade A, or others). In fact, I_1 and i_1 have the same relevance, for clarity, we introduce them separately. Furthermore, c_n $(n = 1, 2, 3\cdots)$ denotes a value in the range. Then a representative value is specified for each of the evaluation result, yielding (10)

$$\mathbf{I}' = \begin{bmatrix} I_1' & I_2' & \cdots & I_n' \end{bmatrix} \tag{10}$$

where $\mathbf{I}'$ is the specific evaluation set, $I_1' = (c_1 + c_2)/2$, $I_2' = (c_2 + c_3)/2, \cdots, I_n' = (c_n + c_{n+1})/2$

(b) Establishing the Evaluation Set of Each Index. For a specific index possibly obtained from some tests or measurements, its evaluation result can be classified into $V_1, V_2, \cdots, V_n$ $(n = 1, 2, 3\cdots)$ in a set $\mathbf{V}$ (see (11)). Similarly, each element in the set $\mathbf{V}$ can be specified in a range (Table 3).

$$\mathbf{V} = \begin{bmatrix} V_1 & V_2 & \cdots & V_n \end{bmatrix} \tag{11}$$

where V_n $(n = 1, 2, 3\cdots)$ denotes the evaluation results of the indices. v_n $(n = 1, 2, 3\cdots)$ represents the description of the evaluation results (e.g., v_1 is excellent, grade A or others). d_n $(n = 1, 2, 3\cdots)$ is a value of the range. It should be noted that the set $\mathbf{I}$ is formed for the target, and set $\mathbf{V}$ for the indices.

Table 2: Range of evaluation results in the set $\mathbf{I}$.

Element	Evaluation result (classification)	Range
I_1	i_1	(c_1, c_2)
I_2	i_2	(c_2, c_3)
I_3	i_3	(c_3, c_4)
I_4	i_4	(c_4, c_5)
$\cdots$	$\cdots$	$\cdots$
I_n	i_n	(c_n, c_{n+1})

Table 3: Range of evaluation results in the set $\mathbf{V}$.

Element	Evaluation result (classification)	Range
V_1	v_1	(d_1, d_2)
V_2	v_2	(d_2, d_3)
V_3	v_3	(d_3, d_4)
V_4	v_4	(d_4, d_5)
$\cdots$	$\cdots$	$\cdots$
V_n	v_n	(d_n, d_{n+1})

Essentially, the evaluation result (or classification), both in $\mathbf{I}$ and $\mathbf{V}$, should be consistent.

(c) Calculating the Index Membership. In this step, a piecewise membership function, to assign a membership ranging from 0 to 1 to each index, is employed (Figure 2), and its expressions are given in (15)–(18). Accordingly, a membership vector, $\mathbf{r}_i$ $(i = 1, 2, 3, \cdots)$, is obtained (see (12)).

$$\mathbf{r}_i = \begin{bmatrix} y_1, y_2, \cdots, y_n \end{bmatrix} \tag{12}$$

where $y_1, y_2, \cdots, y_n$ are the memberships for each evaluation result and n is the number of the evaluation results.

To illuminate the usage of the membership function clearly, we give an example where n=4 (the evaluation set includes four elements and the membership function four parts) in Figure 2. For instance, if the value of the index, P_{12}, is equal to x (Figure 2), then the membership for each evaluation result is y_1, y_2, 0, and 0, respectively. Thus, the membership vector can be expressed as (13). Moreover, there

is a matrix relationship between vector $[a_1 \ a_2 \ a_3 \ a_4]^{\mathrm{T}}$ and vector $[d_2 \ d_3 \ d_4]^{\mathrm{T}}$ (see (14)).

$$\mathbf{r}_i = [y_1 \ y_2 \ 0 \ 0] \tag{13}$$

$$\begin{bmatrix} a_1 \\ a_2 \\ a_3 \\ a_4 \end{bmatrix} = \begin{bmatrix} 0.8 & 0 & 0 \\ 0.5 & 0.5 & 0 \\ 0 & 0.5 & 0.5 \\ 0 & 0 & 1.2 \end{bmatrix} \begin{bmatrix} d_2 \\ d_3 \\ d_4 \end{bmatrix} \tag{14}$$

$$\mu_1(x) = \begin{cases} 1 & x < a_1 \\ \dfrac{x - a_2}{a_1 - a_2} & a_1 \le x \le a_2 \\ 0 & x > a_2 \end{cases} \tag{15}$$

$$\mu_2(x) = \begin{cases} 0 & x < a_1 \\ \dfrac{x - a_1}{a_2 - a_1} & a_1 \le x \le a_2 \\ \dfrac{x - a_3}{a_2 - a_3} & a_2 < x \le a_3 \end{cases} \tag{16}$$

$$\mu_{n-1}(x) = \begin{cases} 0 & x < a_{n-2} \\ \dfrac{x - a_{n-2}}{a_{n-1} - a_{n-2}} & a_{n-2} \le x \le a_{n-1} \\ \dfrac{x - a_n}{a_{n-1} - a_n} & a_{n-1} < x \le a_n \end{cases} \tag{17}$$

$$\mu_n(x) = \begin{cases} 0 & x \le a_{n-1} \\ \dfrac{x - a_{n-1}}{a_n - a_{n-1}} & a_{n-1} \le x \le a_n \\ 1 & x > a_n \end{cases} \tag{18}$$

where $\mu_1, \mu_2, \cdots, \mu_{n-1}, \mu_n$ are piecewise functions, x is the value of an index, and $a_1, a_2, \cdots, a_{n-1}, a_n$ are the parameters defining these functions.

By repeating the procedure stated above, all the membership vectors are calculated for all the indices calculated. Finally, by arranging these membership vectors, the membership matrix, **R**, is expressed as given in (19).

$$\mathbf{R} = [\mathbf{r}_1 \ \mathbf{r}_2 \ \cdots \ \mathbf{r}_i]^{\mathrm{T}} = \begin{bmatrix} r_{11} & r_{12} & \cdots & r_{1n} \\ r_{21} & r_{22} & \cdots & r_{2n} \\ \vdots & \vdots & \ddots & \vdots \\ r_{i1} & r_{i2} & \cdots & r_{in} \end{bmatrix} \tag{19}$$

where r_{in} (i is the number of indices and n is the number of evaluation result) is an element in a membership vector.

(d) Evaluating the Target. By the AHP, the weight matrix, **W**, is obtained. Then a calculated set, **B**, is expressed as in (20).

$$\mathbf{B} = \mathbf{W} \times \mathbf{R} = [b_1 \ b_2 \ \cdots \ b_n] \tag{20}$$

where **R** is the membership matrix and b_n (n is the number of evaluation results) is a specific number, whose value is no more than 1. Eventually, a score of the target is acquired by (21).

$$S = \mathbf{B} \times \mathbf{I}'^{\mathrm{T}} \tag{21}$$

where S is the score, **B** is the calculated set, and $\mathbf{I}'^{\mathrm{T}}$ is the specific evaluation set.

2.3. Fuzzy Analytic Hierarchy Process (FAHP). As stated above, the FAHP is comprised of three components. First, the evaluation target of a project is determined according to the research objective. Second, the AHP model is established. In the model, some essential factors, namely, criteria and indices, which strongly affect the evaluation target are selected, form a multilayer hierarchy model. The aim of this step is to obtain a weight matrix **W**, the link between the AHP and fuzzy method. Finally, the score of the target is acquired and evaluated using the fuzzy method. In this step, the two evaluation sets ($\mathbf{I}'$ and **V**) are set up regarding the target, with each index being the centerpiece. A series of calculations about the membership function and membership matrix **R** are also important. Then the weight matrix, **W**, membership matrix, **R**, and evaluation set, $\mathbf{I}'$, are utilized to obtain the final score of the target. The workflow of the FAHP is shown in Figure 3.

3. Qualitative Evaluation of the GSPG

3.1. Project Overview. The Tongluoshan tunnel, which was control engineered on the Dianlin highway, is located in the Sichuan Province, China. It is 5197 m long and spans 12.7 m. The depth of the shallow-buried section near the Liaojia gully is merely 6–25 m (Figure 4(a)). The lithology in the shallow-buried section is dark gray limestone with a 5–10 cm layer thickness, the thickest of which can reach 30 cm. The rock mass, containing numerous fissures, is strongly weathered, and even small pieces of the rock can be easily split with hands. Moreover, the rock mass is water rich, the permeability rate of which ranges from 30.36 to 65.61 Lu (Section 3.3.2, before grouting in Table 6). Additionally, in the Tongluoshan tunnel, a karst is developed, and a critical water inrush or muddy phenomenon occurs, resulting in a high risk during tunnel construction. The above will pose numerous challenges during construction. Therefore, the GSPG technique was adopted in the shallow-buried section to reinforce the rock mass and prevent water leakage. As shown in Figure 4(b), the GSPG zone, counting a test zone, is 204 m long, where the boreholes are divided into three sections to grout, with a depth of 7 m, 6 m, and 7 m, respectively (Figures 4(b) and 4(c)).

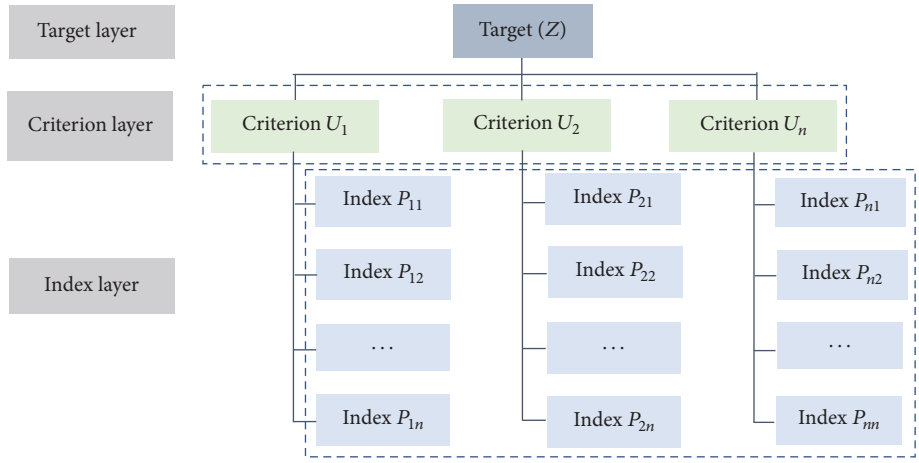

Figure 1: AHP model.

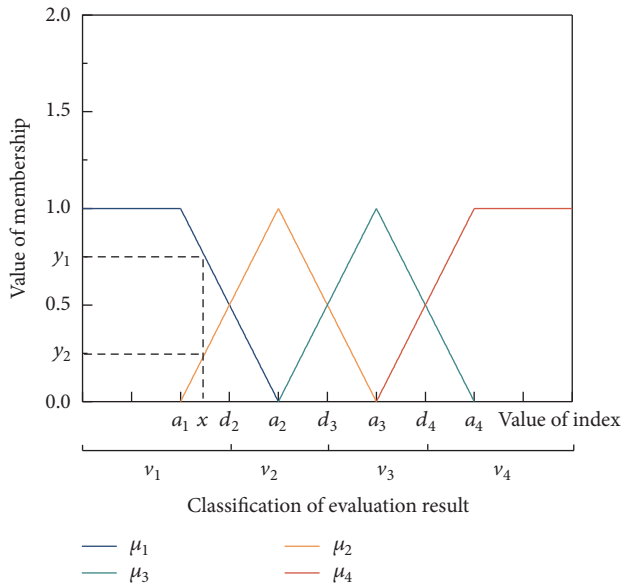

Figure 2: Membership function.

3.2. Design of the GSPG

3.2.1. Layout of the Boreholes. A large inhomogeneity exists in the vertical and horizontal directions in terms of the stratum of the GSPG zone. Consequently, the arrangement of the grouting holes was in the form of a quincunx and the horizontal and vertical distances between two holes are 2 m (not all the holes are presented in Figure 5). The holes have two types: grouting holes and test holes (i.e., holes before test and holes after test), with a diameter of 0.11 m.

The grouting process was performed in three orders: primary, secondary, and tertiary grouting, represented by dark blue, orange, and green, respectively. The test data of the GSPG were obtained from five pairs of test holes (denoted by red). The holes before test were implemented to obtain the rock mass parameters before grouting, and the holes after test the parameters after grouting. The rock mass parameters before and after grouting were compared to qualitatively evaluate the quality of the GSPG.

3.2.2. GSPG Parameters. The GSPG parameters are comprised of the grouting pressure, diffusion radius of the slurry, and grouting volume per borehole. In case of the grouting pressure, a high grouting pressure can make the slurry penetrate the stratum rapidly, and it is beneficial to precipitate the moisture of the slurry to accelerate its cementing process. However, an extremely high grouting pressure may split the rock mass, resulting in slurry loss [23] and prompting the uplift of the ground surface [4]. In this GSPG, the grouting pressure was 1.0–1.5 MPa, with mulling over the construction conditions, such as the tunnel depth, layout of the boreholes, and the weathering degree of the rock mass [24]. The diffusion radius of the slurry is related to numerous factors such as the rheological behavior of the slurry [4], grouting time, and grouting pressure. For overlapping the diffusion range of the slurry, the diffusion radius is determined to be 1.3 m based on the layout of the holes and engineering experience.

More significantly, owing to a strongly weathered rock mass and highly developed groundwater, the slurry is easily diluted or even washed away, causing slurry loss. Moreover, the presence of numerous fissures in the rock mass in the test zone also facilitates slurry loss [23]. Hence, the slurry loss cannot be disregarded.

In general, to prevent the slurry from being highly diluted, relatively high concentrations are used in strongly weathered zones. If the groundwater is highly developed, the cement slurry needs a longer time to solidify, producing a worse effect of GSPG. Under this condition, adding some polymers to the slurry could decrease the slurry loss [25], thereby improving the GSPG quality.

Given the complex geological conditions, however, the loss of the slurry tends to become difficult to measure before grouting. According to the engineering experience, the volume of the slurry should be more than the designed value to ensure the grouting quality.

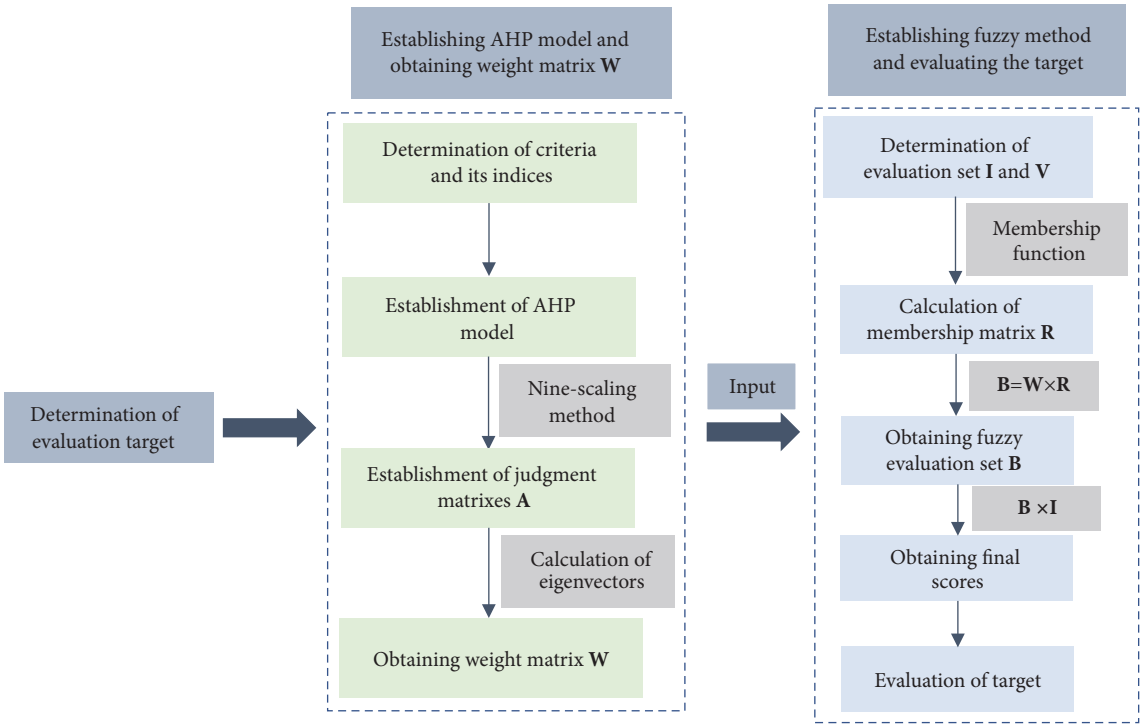

Figure 3: Comprehensive evaluation process of the FAHP.

First, the grouting volume per borehole is estimated preliminarily based on (22) [26],

$$Q = \pi R^2 Hn \cdot m \tag{22}$$

where Q is the grouting volume per borehole, R is the diffusion radius, H is the borehole depth, n is the porosity of the rock mass, having a value 1%–5%, and m is a factor, related to A, β, and α, as expressed in in (23).

$$m = \frac{A\beta}{\alpha} \tag{23}$$

where A is a factor relating to the grouting loss, generally having a value 1.2–1.5; β is a factor relating to the filling degree, having a value 0.8–0.9; and α is a factor relating to the consolidation rate of the slurry, having a value 0.5–0.95.

Second, the finishing standard of grouting is determined. It stipulates that the grouting flow is 20–35 L/min, with the grouting pressure reaching the final pressure and maintaining for 20–30 min [26]. It should be noted that (22) is merely used for estimating the amount of the slurry required and to ensure that the slurry can completely fill the fissures and cavities. Therefore, the finishing standard should be employed.

Finally, in this GSPG, the grouting volume per borehole was estimated preliminarily using (24).

$$\begin{aligned} m &= 1.35 \times \frac{0.85}{0.73} = 1.57 \\ Q &= \pi \times 1.3^2 \times 20 \times 4.5\% \times 1.57\text{m}^3 = 7.43\text{m}^3 \end{aligned} \tag{24}$$

In practice, to render the GSPG more effective, we strictly followed the standard (the final grouting pressure exceeded the maximum designed value of 1.5 MPa, with the grouting flow being 20–35 L/min and the grouting pressure maintaining for 30 min) and add sodium silicate (water glass) to the slurry, with a concentrate of 35 Bé and a volume proportion of 3%–5%. The grouting volume per borehole in the test zone is as shown in Table 4. The practical grouting volume in borehole #3 is less than the estimated value of 7.43 m^3, whereas those in #1 and #2 almost equal the value and those in #4 and #5 exceed the value. The excess rates (i.e., a rate that reflects that the practical grouting volume exceeds the designed one) of the latter are 12% and 13%, respectively, normal values that meet the requirement of the standard [26].

3.3. Qualitative Evaluation of the GSPG. Owing to the complex geology conditions, the GSPG quality is required quantitative evaluation using the FAHP (Section 4) where the index values are required. Therefore, in this section, a series tests was performed to obtain the index values. Furthermore, to verify the results from the FAHP, the results from the tests were preliminary used for qualitatively evaluating the GSPG quality from the three aspects.

In general, the objective of a GSPG is twofold: to reduce the permeability rate and improve quality of the surrounding rock. Therefore, the tests can be performed based on the three aspects namely, the integrity, continuity, and sturdiness of the rock mass.

3.3.1. Integrity Test. When a broken rock is cemented by the slurry, the integrity of the grouted rock mass improves.

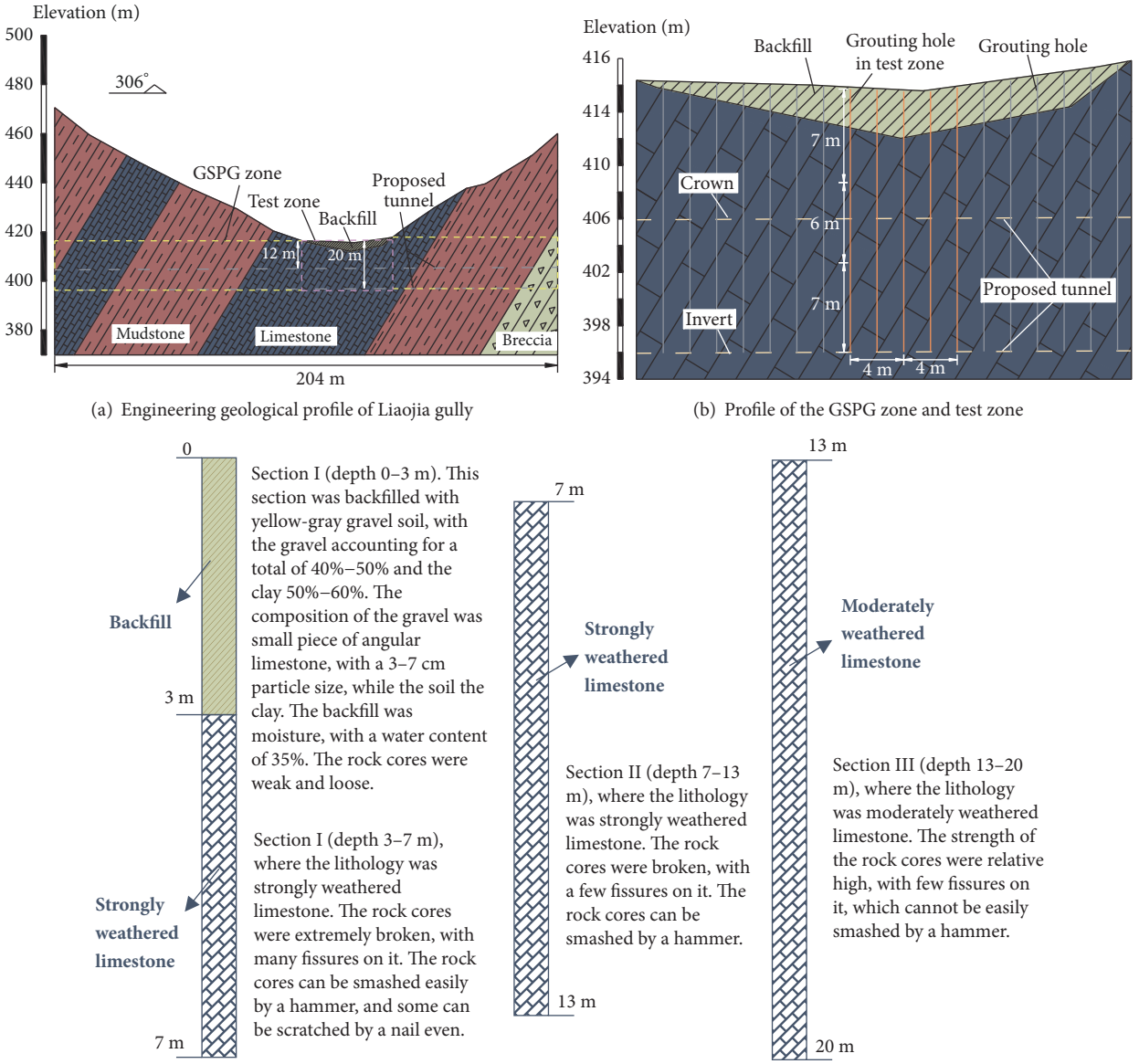

(a) Engineering geological profile of Liaojia gully

(b) Profile of the GSPG zone and test zone

(c) Log data in the test zone

Figure 4: Profile of the grouting project.

Table 4: Grouting volume per borehole at the three sections.

Depth (m)	Number of boreholes				
	1	2	3	4	5
0–7	4.50	4.48	4.17	4.67	5.31
7–13	1.47	1.52	1.28	1.64	1.99
13–20	1.53	1.48	1.72	2.01	1.13
Total	7.50 (0.9%)	7.48 (0.7%)	7.17	8.32 (12%)	8.43 (13%)

Please note that "(0.9%)", "(0.7%)", "(12%)", and "(13%)" are the excess rates.

The integrity test is generally implemented by an ultrasonic method [27]. The sound velocity is related to the type of rock mass, physical and mechanical parameters, weathered degree, and density degree [28, 29]. A dense and complete grouted rock mass implies a high sound velocity.

The integrity tests were implemented in both single boreholes (J1, J2, J3, J4, J5) (Figure 6(a)) and double boreholes (J2–J1, J2–J3, J2–J5) (Figure 6(b)). A transmitter and receiver were installed on a probe with a recorder on the ground. The single-borehole tests reflect the rock mass quality near

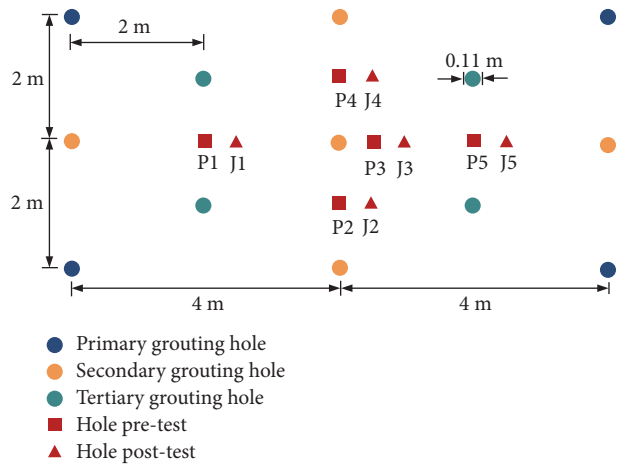

Figure 5: Schematic of grouting and test holes arrangement in the test area (strike: 306°).

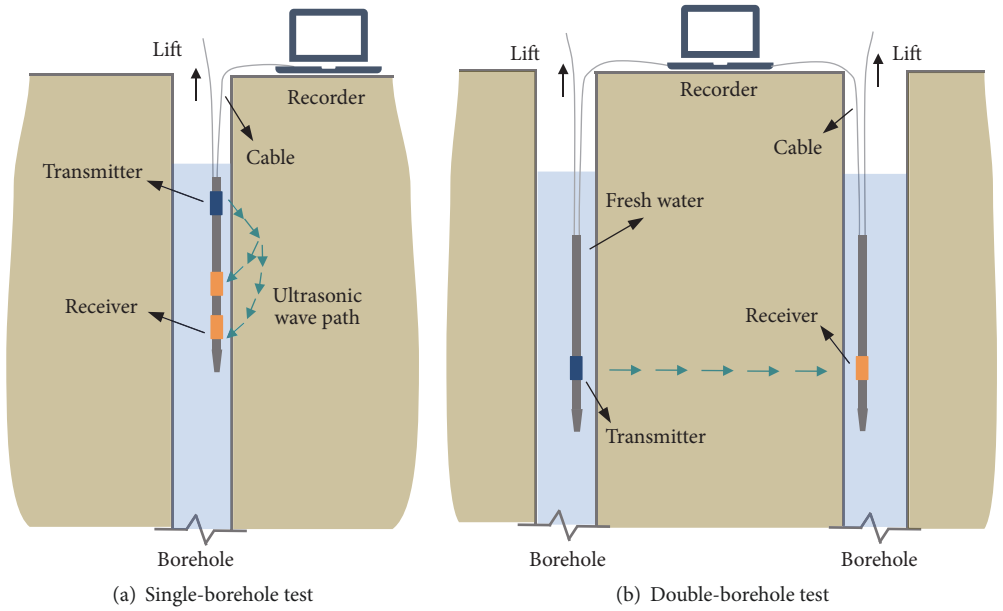

Figure 6: Schematic of the test of ultrasonic waves.

a borehole, whereas the double-borehole tests represent that between two boreholes.

In the single-borehole tests, first, the ultrasonic data of the five boreholes are missing at a depth of 0–10 m (Figure 7), indicating that the fissures are highly developed, and the water leakage is serious before grouting. After grouting, the ultrasonic data are complete at a depth of 0–10 m, indicating that the fissures are filled by the slurry. Second, before and after the grouting, the average sound velocity is 2273 m/s and 2639 m/s, respectively, which is increased by 16%. Both the facets indicate that the near-borehole quality of the rock mass is markedly improved.

In the double-borehole tests, first, the ultrasonic data are missing at depths of 0–10 m before grouting (Figure 8), thereby indicating the fissures between the two boreholes are developed at the depth range, and the permeability rate of the stratum is high. After grouting, the data between 0 and 10 m are complete, thereby suggesting that the fissures are blocked by the slurry and the permeability is much lower than before. Second, the average sound velocity is 3119 m/s after the grouting, rising by 7% relative to 2909 m/s. The two aspects reflect that the between-borehole quality of the rock mass is boosted.

Both the single-borehole and double-borehole teats reflect the improvement degree of the rock mass. The latter, however, is slightly higher than the former. This is partly because the ultrasonic wave is not sensitive to the fissures particularly those that are small. It tends to transmit in a complete rock rather than in the fissure-spreading, when it transmits in the stratum between two boreholes. In terms of the integrity, the two tests reveal that the GSPG is effective.

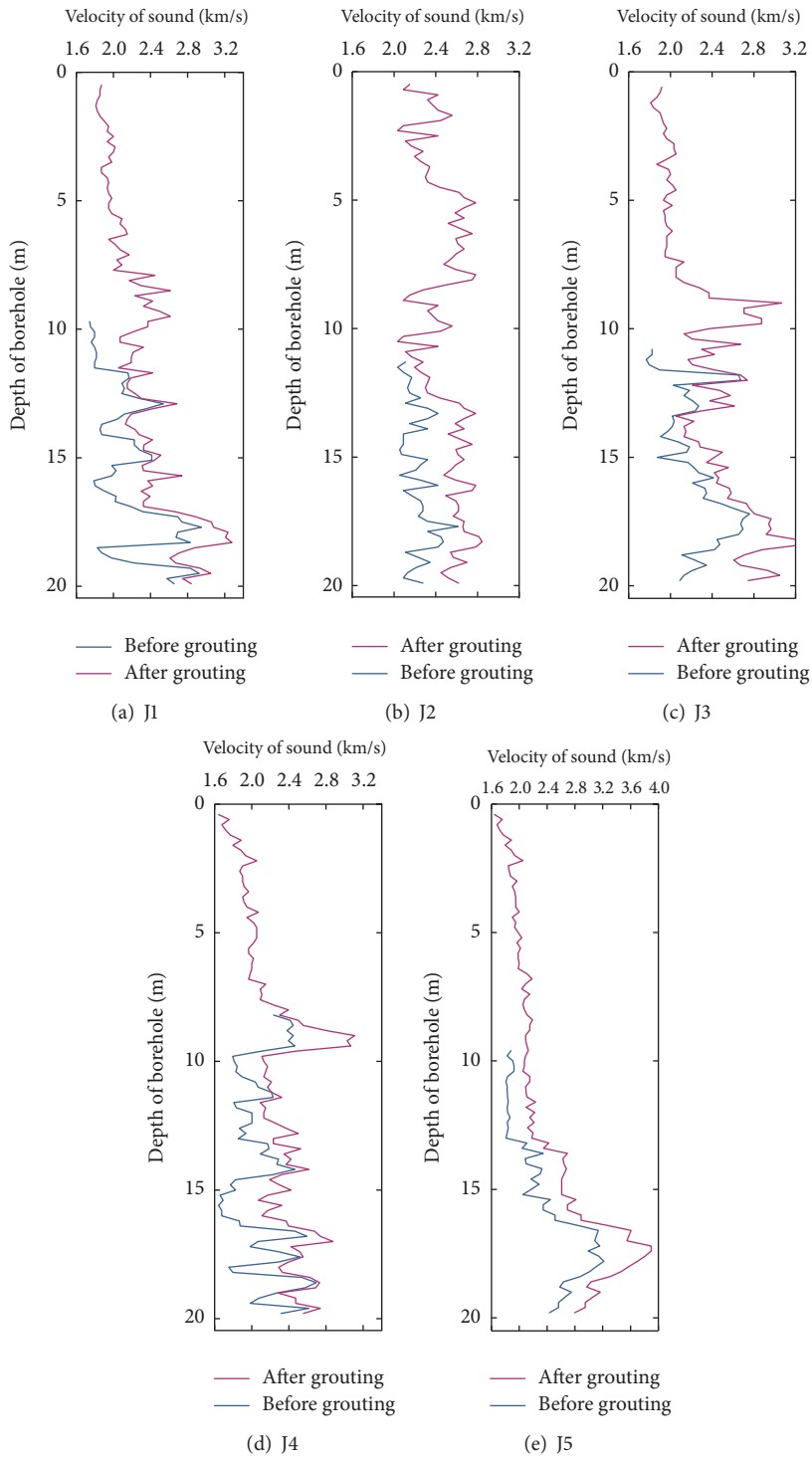

Figure 7: Sound velocity at different depths in the single-borehole tests.

3.3.2. Continuity Test. The continuity test generally entails an evaluation via the water pressure test [30]. An in situ penetration test is conducted in a borehole; it is the most commonly used method to determine the permeability rate of a rock mass (Figure 9), whose unit is Lugeon as proposed by Lugeon [31]. A Lugeon is defined as the water loss of 1 L/min per meter length of the test section at an effective pressure of 1 MPa.

As for the continuity test, the key indices include four types (i.e., A, B, C, and D) of the p-Q (i.e., p, grouting pressure; Q, grouting flow) curve and the permeability rate of the rock mass [30]. The four types of the p-Q curve are used

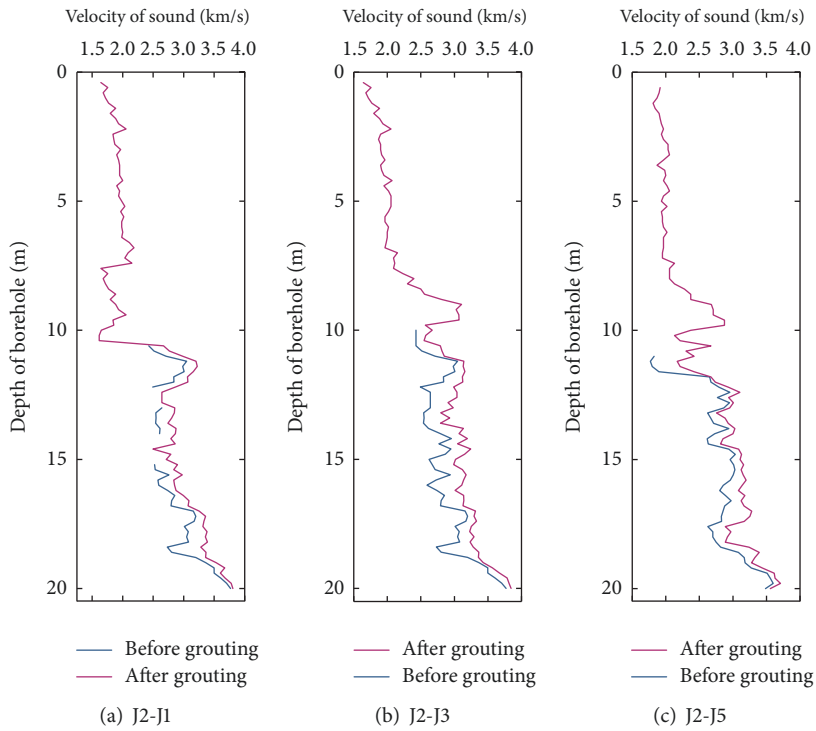

Figure 8: Sound velocity at different depths in the double-borehole tests.

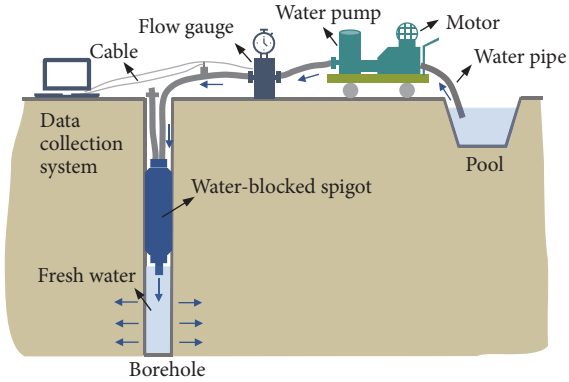

Figure 9: Schematic of the water pressure test.

for depicting the fissure conditions during grouting. Type A is an excellent one, followed by types B and C—both are acceptable—and type D, a bad one. The definitions of the curve types are illustrated in Table 5.

As shown in Figure 5, the test holes have five pairs, each of which are divided into three sections (0–7, 7–13, and 13–20 m deep, respectively) from top to bottom (Figure 4(c)). The types of the p-Q curve and permeability rate, in all the sections, are listed in Table 6.

As shown in Table 6, before grouting, the permeability rate is 45.78 Lu on an average, a relatively high value. The curve types are mainly classified as types D accounting for a total of 73% (i.e., the total number of samples is 15, and the number of type D is 11; thus, the calculated percentage is 73%) (Figure 10). Types A, B, and C have an extremely low proportion, accounting for a total of 7%, 7%, and 13%, respectively. Both indicate that the fissures of the rock mass are highly developed.

After grouting, the permeability rate is 4.30 Lu (very low) on average, which decreases by approximately 90%. Then the proportion of type A and B increases to 60% and 27%, respectively, whereas that of type D is reduced to 6%. These results indicate that a considerable number of fissures are filled, and most of them would not be split when grouting. Therefore, in terms of the continuity, the GSPG is effective.

3.3.3. Sturdiness Test. In the sturdiness test, the unconfined compressive strength of the rock samples [32] was determined. The samples were obtained at a depth of 13–20 m in the holes before test and after test (i.e., P1–P5, J1–J5), where the lithology was moderately weathered limestone. The test data are listed in Table 7. The unconfined compressive strength of the rock samples improves by 13% on average, indicating that the GSPG is effective in terms of the sturdiness.

4. Quantitative Evaluation of the GSPG

These tests can only be utilized to qualitatively evaluate the quality of a GSPG, with the results being effective or ineffective. Hence, an FAHP based on the three facets was performed to quantitatively evaluate the quality, obtaining the quality classification (as well as the final score) of the GSPG.

Table 5: Five curve types of the water pressure test.

Curve types	Relationships between pressure and flow	Characteristics of curve types	Depictions
Type A	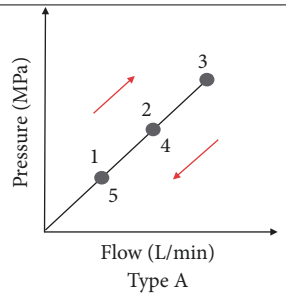 Type A	Two curves (1-2-3 and 3-4-5) are straight lines originating at (0, 0) and are coincident	An excellent condition, where the seepage form is laminar flow. Fissures do not change throughout the test.
Type B	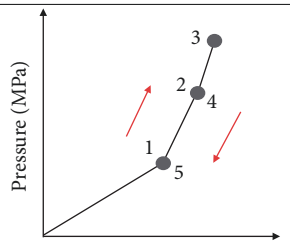 Type B	Two curves (1-2-3 and 3-4-5) converge to the Q-axis and coincide	An acceptable condition, where the seepage form is turbulent flow. Fissures do not change throughout the test.
Type C	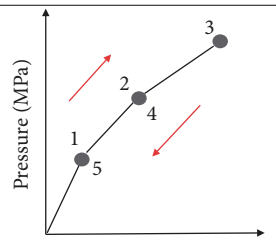 Type C	Two curves converge (1-2-3 and 3-4-5) to the p-axis and coincide	An acceptable condition where the fissure form changes and the permeability of the rock mass increases as the test pressure increases, but the change is temporary and reversible. As the pressure decreases, the fissures return to the original form, showing a behavior of elastic expansion.
Type D	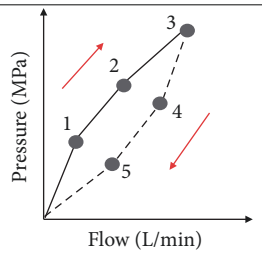 Type E	Curve 1-2-3 converges to the p-axis and does not coincide with curve 3-4-5	A bad condition, where the fissure form changes and the permeability of rock increases as the pressure increases. This change is permanent and irreversible. The flow is significantly increased and cannot be restored to its original form, indicating fissures are split.

Table 6: Permeability rate and curve types obtained from the five pairs of the test holes.

Depth (m)	Before or after grouting	Number of boreholes				
		1	2	3	4	5
0–7	Before	53.97/D	50.91/D	65.61/D	62.13/D	53.78/B
	After	4.90/A	5.12/A	4.69/B	4.67/B	4.72/A
7–13	Before	47.12/D	45.50/D	42.00/D	41.18/D	46.21/C
	After	4.31/A	4.26/B	4.81/C	5.18/D	4.33/A
13–20	Before	34.42/C	30.36/D	36.16/D	41.10/D	36.19/A
	After	3.44/A	3.69/A	3.21/A	3.96/B	3.15/A

Note: the unit of the permeability rate is Lu.

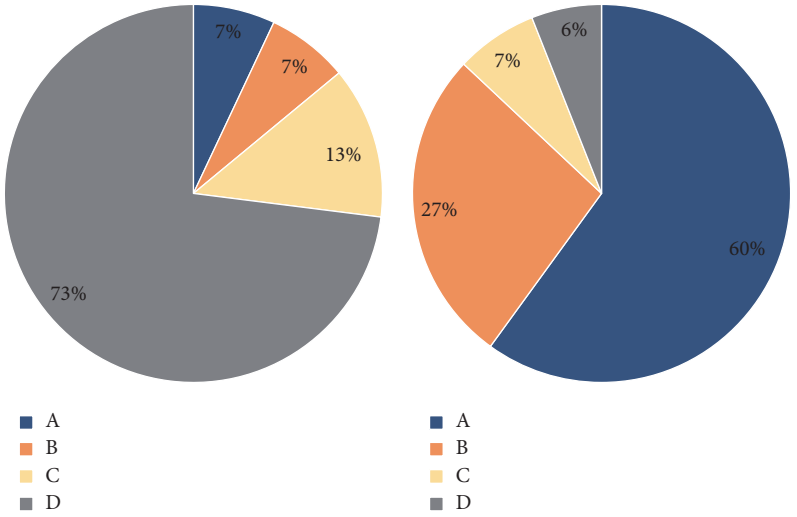

(a) Before grouting (b) After grouting

Figure 10: Proportion of each curve types before and after grouting.

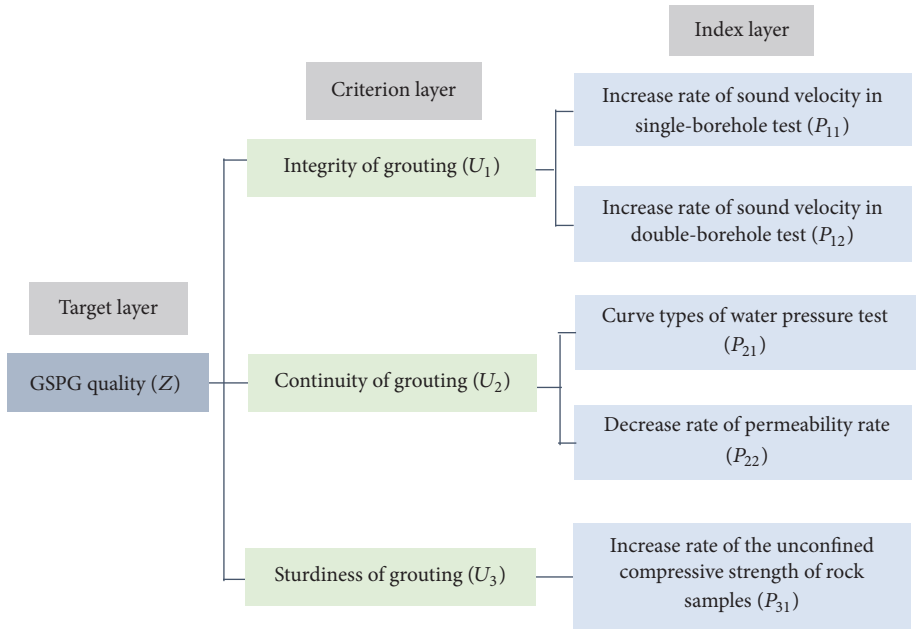

Figure 11: AHP model for the GSPG.

4.1. Analytic Hierarchy Process (AHP)

(a) AHP Model. According to Section 2.1 (a), first, the "GSPG quality" was specified on the target layer. The objective of the GSPG is twofold: to improve the quality of the rock mass and reduce the permeability rate of the rock mass. Thus, three aspects, integrity, continuity, and sturdiness, were selected as the criteria on the criterion layer in the AHP model. Then the five sublayer factors, the indices, which were obtained from the three tests, were determined on the index layer. Consequently, a three-layer AHP model was established (Figure 11).

(b) Devising the Judgment Matrices. In this GSPG project, compared with the continuity and sturdiness, the integrity was the most essential factor because it comprehensively reflected the quality of the rock mass and also reflected the other two factors to some degree. By comparing the importance of the criteria U_1, U_2, and U_3, on the criterion layer, the judgment matrix $\mathbf{A}_Z$ was obtained. Similarly, by

Table 7: Increase rate of the unconfined compressive strength of the rock samples before and after grouting.

Number of rock samples	Before grouting (MPa)	After grouting (MPa)	Increase rate of unconfined compressive strength of the rock samples (%)
P1-1	10.5	12.3	17.1
J1-2	13.5	15.3	13.3
P2-1	19.2	21.2	10.4
J2-2	21.7	23.4	7.8
P3-1	15.3	17.1	11.8
J3-2	14.1	16.3	15.6
P4-1	13.2	15.6	18.2
J4-2	18.3	20.6	12.6
P5-1	17.1	19.4	13.5
J5-2	18.7	20.3	8.6

Table 8: Evaluation results of the target and their scores.

Elements	Evaluation results	Scores
I_4	Excellent	>90
I_3	Good	80–90
I_2	Moderate	60–79
I_1	Bad	<60

comparing the importance of (P_{11} and P_{12}) and (P_{21} and P_{22}), the judgment matrices $\mathbf{A}_{U_1}$ and $\mathbf{A}_{U_2}$ were obtained. Because there was merely one index on the sublayer of U_3, the element in matrix $\mathbf{A}_{U_3}$ is 1. The four judgment matrices are shown in (25).

$$\begin{aligned}
\mathbf{A}_Z &= \begin{bmatrix} 1 & 2 & 3 \\ \frac{1}{2} & 1 & 2 \\ \frac{1}{3} & \frac{1}{2} & 1 \end{bmatrix}, \\
\mathbf{A}_{U_1} &= \begin{bmatrix} 1 & 2 \\ \frac{1}{2} & 1 \end{bmatrix}, \\
\mathbf{A}_{U_2} &= \begin{bmatrix} 1 & 2 \\ \frac{1}{2} & 1 \end{bmatrix}, \\
\mathbf{A}_{U_3} &= [1]
\end{aligned} \tag{25}$$

(c) Determining the Weight Matrix. Using MATLAB programming, the normalized eigenvectors of the four judgment matrices are given in (26). The weight matrix, **W**, is derived from (8), as shown in (27).

$$\begin{aligned}
\mathbf{e}_Z &= [0.54 \quad 0.30 \quad 0.16]^{\mathrm{T}} \\
\mathbf{e}_{U_1} &= [0.67 \quad 0.33]^{\mathrm{T}} \\
\mathbf{e}_{U_2} &= [0.67 \quad 0.33]^{\mathrm{T}} \\
\mathbf{e}_{U_3} &= [1]^{\mathrm{T}}
\end{aligned} \tag{26}$$

$$\mathbf{W} = [0.36 \quad 0.18 \quad 0.20 \quad 0.10 \quad 0.16] \tag{27}$$

where $\mathbf{e}_Z$, $\mathbf{e}_{U_1}$, $\mathbf{e}_{U_2}$, and $\mathbf{e}_{U_3}$ are the normalized eigenvectors of the four judgment matrices.

4.2. Fuzzy Method

(a) Establishing the Evaluation Set of the Target. In this GSPG project, we classify the quality of the GSPG into four categories, namely, excellent, good, moderate, and bad [21], and provide the range (score) of each category (Table 8). The four-element evaluation set, **I**, and the specific evaluation set, $\mathbf{I}'$, are established as expressed in (28) and (29)

$$\mathbf{I} = [I_4 \quad I_3 \quad I_2 \quad I_1] \tag{28}$$

$$\mathbf{I}' = [30 \quad 70 \quad 85 \quad 95] \tag{29}$$

where **I** is the evaluation set of the target and I_4, I_3, I_2, and I_1 are the categories of the GSPG quality, which represent "Excellent", "Good", "Moderate", and "Bad," respectively.

(b) Establishing the Evaluation Set of Each Index. The evaluation sets of the indices from the field tests should be consistent with the evaluation set of the target. Therefore, the evaluation sets are also compromised of four categories: Excellent, Good, Moderate, and Bad (see (30)). The category range of each index, however, is different from one another (Table 9).

$$\begin{aligned}
\mathbf{V} &= [V_4 \quad V_3 \quad V_2 \quad V_1] \\
&= [\text{Excellent} \quad \text{Good} \quad \text{Moderate} \quad \text{Bad}]
\end{aligned} \tag{30}$$

Table 9: Definitions of the evaluation results for each index.

Index	Symbol	Range of each evaluation result				Test data
		Excellent	Good	Moderate	Bad	
Increase rate of sound velocity in single-borehole test (%)	P_{11}	>15	10–15	5–10	<5	16
Increase rate of sound velocity in double-borehole test (%)	P_{12}	>15	10–15	5–10	<5	7
Curve types of water pressure test	P_{21}	A	B	C	D	A: 60%, B:27%, C: 7%, D: 7%
Decrease rate of permeability rate (%)	P_{22}	>80	60–80	40–60	<40	90
Increase rate of the unconfined compressive strength of rock samples (%)	P_{31}	>15	10–15	5–10	<5	13

where $\mathbf{V}$ is the evaluation set of each index and V_4, V_3, V_2, and V_1 are the categories of the GSPG quality, which represent "Excellent", "Good", "Moderate", and "Bad," respectively.

(c) Calculating Index Membership. Based on the test data (Table 9) and membership function (Figure 2), the memberships of the indices P_{11}, P_{12}, P_{22}, and P_{31} are calculated using the process stated in Section 2.2(c) and are shown in Figure 12. As for index P_{21}, its range of each evaluation result is a discrete data, i.e., A, B, C, and D, and therefore, the test data are directly used as the membership. Finally, by arranging the membership of each index in order, the membership vector, $\mathbf{r}_i$, and the matrix, $\mathbf{R}$, are yielded (see (31) and (32)).

$$\begin{aligned}\mathbf{r}_1 &= [0 \;\; 0 \;\; 0.36 \;\; 0.64]\\ \mathbf{r}_2 &= [0.14 \;\; 0.86 \;\; 0 \;\; 0]\\ \mathbf{r}_3 &= [0.07 \;\; 0.07 \;\; 0.27 \;\; 0.60]\\ \mathbf{r}_4 &= [0 \;\; 0 \;\; 0.23 \;\; 0.77]\\ \mathbf{r}_5 &= [0 \;\; 0 \;\; 0.91 \;\; 0.19]\end{aligned} \tag{31}$$

$$\mathbf{R} = \begin{bmatrix} 0 & 0 & 0.36 & 0.64 \\ 0.14 & 0.86 & 0 & 0 \\ 0.07 & 0.07 & 0.27 & 0.60 \\ 0 & 0 & 0.23 & 0.77 \\ 0 & 0 & 0.91 & 0.19 \end{bmatrix} \tag{32}$$

(d) Evaluating the Quality of the GSPG. Using the AHP, the weight of each index is incorporated in the weight matrix, $\mathbf{W}$, and the membership of these indices, required in each evaluation result, is expressed by the membership matrix, $\mathbf{R}$. By (20) and (21), the final score of quality the GSPG is obtained (see (33)).

$$S = \mathbf{W} \times \mathbf{R} \times \mathbf{I}'^{\mathrm{T}} = [0.36 \;\; 0.18 \;\; 0.20 \;\; 0.10 \;\; 0.16] \begin{bmatrix} 0 & 0 & 0.36 & 0.64 \\ 0.14 & 0.86 & 0 & 0 \\ 0.07 & 0.07 & 0.27 & 0.60 \\ 0 & 0 & 0.23 & 0.77 \\ 0 & 0 & 0.91 & 0.19 \end{bmatrix} [30 \;\; 70 \;\; 85 \;\; 95]^{\mathrm{T}} = [0.0392 \;\; 0.1688 \;\; 0.3522 \;\; 0.4578] \times \begin{bmatrix} 30 \\ 70 \\ 85 \\ 95 \end{bmatrix} = 86.42 \tag{33}$$

where S is the final score, $\mathbf{W}$ is the weight matrix, $\mathbf{R}$ is the membership matrix, and $\mathbf{I}'^{\mathrm{T}}$ is the specific evaluation set. As a result, the final score of the quality of the GSPG was 86.42, which can be classified as "Good" in accordance with Table 8.

5. Conclusions

The FAHP was performed to quantitatively evaluate the quality of GSPG in this study. To qualitatively evaluate the quality of the GSPG and obtain the required data in the FAHP, a series of field tests were also implemented.

The integrity test results showed that the sound velocity in the single-borehole tests and the double-borehole tests increased by 16% and 7%, respectively. The continuity test results showed that the curve types were primarily type A, accounting for a total of 60% after grouting, with the permeability rate decreased by approximately 90%. Concurrently, the sturdiness test result showed that

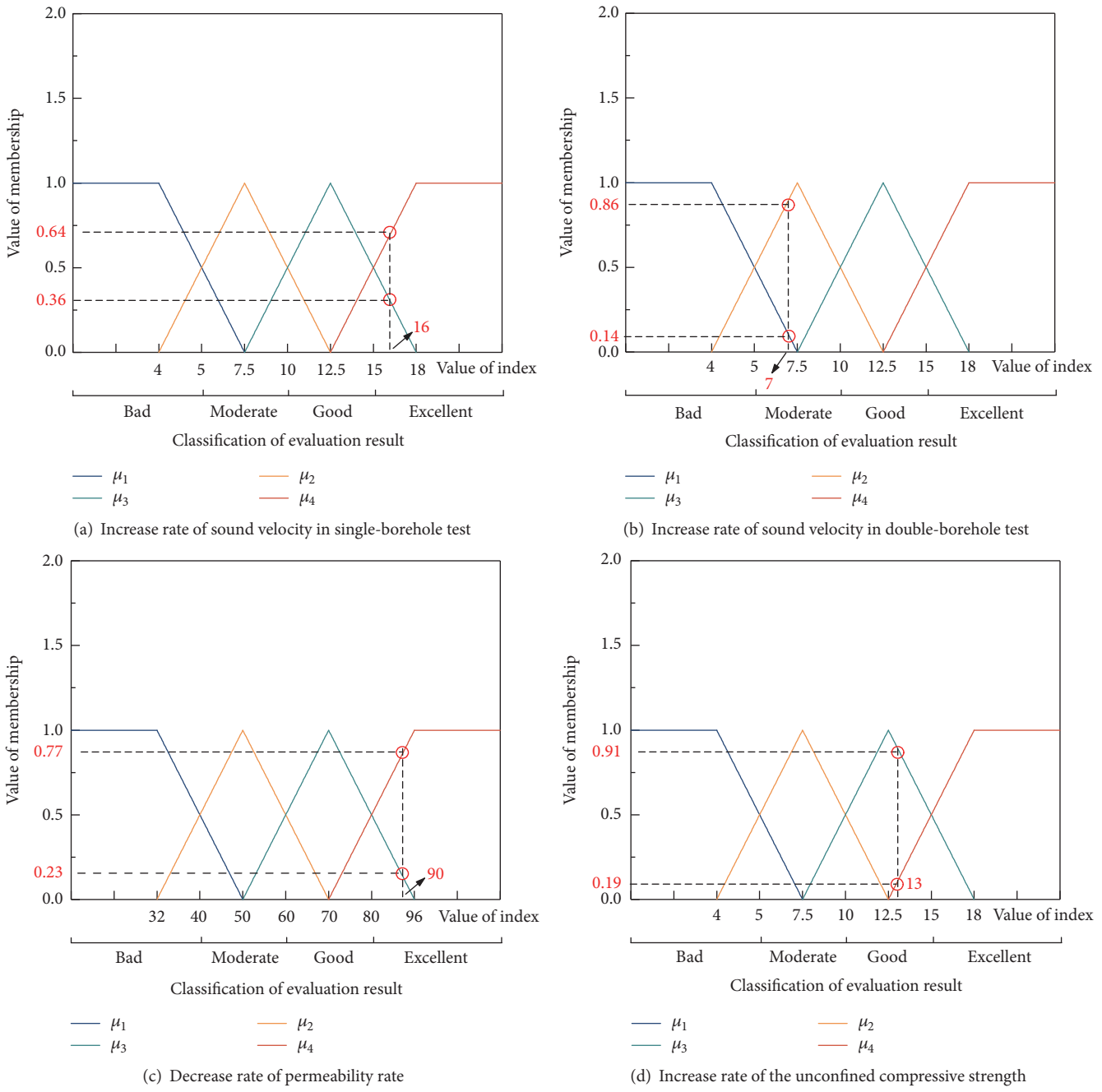

Figure 12: Calculation of the four index memberships.

the unconfined compressive strength of the rock samples increased by approximately 13%. These results indicated that the fissures were effectively filled and that the rock performance was improved by the GSPG, thereby suggesting that the GSPG was effective.

Based on the three aspects and five indices, the FAHP was conducted to quantitatively evaluate the quality of the GSPG. The results showed that the final score of the GSPG was 86.42, which could be classified as "Good". Moreover, the results from the FAHP were consistent with that from the field tests; thus, verifying that the FAHP was reliable and that it could be applied to the quality evaluation of the GSPG. With the qualitative and quantitative evaluations being conducted comprehensively, this quality evaluation of the GSPG provided a frame of reference for analogous engineering.

Data Availability

The test data used to support the findings of this study are available from the corresponding author [Hua Xu] upon request.

Conflicts of Interest

The authors declare that there are no conflicts of interest regarding the publication of this paper.

Acknowledgments

This study is financially supported by the National Key Research and Development Program of China (2016YFB1200401) and the Western Construction Project of the Ministry of Transport (Grant no. 2015318J29040). This support is gratefully acknowledged.

References

[1] N. Shrivastava and K. Zen, "An experimental study of compaction grouting on its densification and confining effects," *Geotechnical and Geological Engineering*, vol. 36, no. 2, pp. 983–993, 2018.

[2] D. Y. Chen, N. Zhang, M. W. Zhang et al., "Application and evaluation of ground surface pre-grouting reinforcement for 800-m-deep underground opening through large fault zones," *Arabian Journal of Geosciences*, vol. 10, no. 13, Article ID 285, 20 pages, 2017.

[3] Q. Zhang, P. Li, G. Wang et al., "Parameters optimization of curtain grouting reinforcement cycle in yonglian tunnel and its application," *Mathematical Problems in Engineering*, vol. 2015, Article ID 615736, 15 pages, 2015.

[4] Z.-F. Wang, J. S. Shen, and W.-C. Cheng, "Simple method to predict ground displacements caused by installing horizontal jet-grouting columns," *Mathematical Problems in Engineering*, vol. 2018, Article ID 1897394, 11 pages, 2018.

[5] J. C. Ni and W.-C. Cheng, "Field response of high speed rail box tunnel during horizontal grouting," *Journal of Testing and Evaluation*, vol. 43, no. 2, pp. 398–413, 2015.

[6] X. Li, Q. Zhang, X. Zhang, X. Lan, C. Duan, and J. Liu, "Detection and treatment of water inflow in karst tunnel: a case study in daba tunnel," *Journal of Mountain Science*, vol. 15, no. 7, pp. 1585–1596, 2018.

[7] J. C. Ni and W.-C. Cheng, "Quality control of double fluid jet grouting below groundwater table: case history," *Soils and Foundations*, vol. 54, no. 6, pp. 1039–1053, 2014.

[8] W. Qing-biao, Z. Qing-kai, S. Tang-sha et al., "The rheological test and application research of glass fiber cement slurry based on plugging mechanism of dynamic water grouting," *Construction and Building Materials*, vol. 189, pp. 119–130, 2018.

[9] W. M. Roman, A. N. Hockenberry, J. N. Berezniak, D. B. Wilson, and M. A. Knight, "Evaluation of grouting for hydraulic barriers in rock," *Environmental and Engineering Geoscience*, vol. 19, no. 4, pp. 363–375, 2013.

[10] E. N. Magoto, *Quantifiying the effectiveness of a grout curtain using a laboratory-scale physical model [MSc Thesis]*, University of Kentucky, Lexington, Ky, USA, 2014.

[11] J. Zadhesh, F. Rastegar, F. Sharifi, H. Amini, and H. M. Nasirabad, "Consolidation grouting quality assessment using artificial neural network (ANN)," *Indian Geotechnical Journal*, vol. 45, no. 2, pp. 136–144, 2015.

[12] F. K. Ewert, "Evaluation and interpretation of water pressure tests," in *Grouting in the Ground*, pp. 141–162, Thomas Telford, London, UK, 1994.

[13] M. Chen, W. Lu, W. Zhang, P. Yan, and C. Zhou, "An analysis of consolidation grouting effect of bedrock based on its acoustic velocity increase," *Rock Mechanics and Rock Engineering*, vol. 48, no. 3, pp. 1259–1274, 2015.

[14] H. F. Xu, H. S. Geng, F. Chen et al., "Strength assessment of broken rock postgrouting reinforcement based on initial broken rock quality and grouting quality," *Mathematical Problems in Engineering*, vol. 2017, Article ID 3651765, 14 pages, 2017.

[15] T. Li and S. Long, "Grout assessment of plastic ducts in prestressed structures with an HHT-based method," *Construction and Building Materials*, vol. 180, pp. 35–43, 2018.

[16] T. L. Saaty, "A scaling method for priorities in hierarchical structures," *Journal of Mathematical Psychology*, vol. 15, no. 3, pp. 234–281, 1977.

[17] T. L. Saaty, "Decision making with the analytic hierarchy process," *International Journal of Services Sciences*, vol. 1, no. 1, pp. 83–98, 2008.

[18] L. A. Zadeh, "Fuzzy set," *Information and Control*, vol. 8, no. 3, pp. 338–353, 1965.

[19] J. S. Xu, H. Xu, R. F. Sun et al., "Seismic risk evaluation for planning mountain tunnel using ET and ET-based improved AHP," *Journal of Mountain Science*, 2019.

[20] G. Fan, D. Zhong, F. Yan, and P. Yue, "A hybrid fuzzy evaluation method for curtain grouting efficiency assessment based on an AHP method extended by D numbers," *Expert Systems with Applications*, vol. 44, pp. 289–303, 2016.

[21] J. Zhang and J. Zhao, "Application of analytic hierarchy process in choice of dam foundation curtain grouting form," *Water Resources and Power*, vol. 27, no. 3, pp. 124–146, 2009.

[22] H. Xu, P. Zhang, J. N. Cheng et al., "Evaluation and application of ground surface pre-grouting," in *Proceedings of the in Mountain Tunnels*, Philadelphia, Pennsylvania, 2019.

[23] Q. Cui, Y. Xu, S. Shen, Z. Yin, and S. Horpibulsuk, "Field performance of concrete pipes during jacking in cemented sandy silt," *Tunnelling and Underground Space Technology*, vol. 49, pp. 336–344, 2015.

[24] DL/T5148, *Technical Specification for Cement Grouting Construction of Hydraulic Structures*, Professional standard of the People's Republic of China, China Electric Power Press, Beijing, China, 2012.

[25] W. Cheng, J. C. Ni, A. Arulrajah, and H. Huang, "A simple approach for characterising tunnel bore conditions based upon pipe-jacking data," *Tunnelling and Underground Space Technology*, vol. 71, pp. 494–504, 2018.

[26] YSJ211-92, *Specification for grouting*, Xi'an Jiaotong Press, Xi'an, China, 1993.

[27] CECS21, *Technical specification for inspection of concrete defects by ultrasonic method*, Professional Standard of the People's Republic of China, China Association for Engineering Construction Standardization, Beijing, China, 2000.

[28] Z. F. Fan, J. C. Zhang, and H. Xu, "Transmission of normal p-wave across a single joint based on g-λ model," *Shock and Vibration*, vol. 2019, Article ID 8240586, 10 pages, 2019.

[29] Z. Fan, J. Zhang, and H. Xu, "Theoretical study of the dynamic response of a circular lined tunnel with an imperfect interface subjected to incident SV-waves," *Computers & Geosciences*, vol. 110, pp. 308–318, 2019.

[30] DL/T5331, *Code for water pressure test in borehole for hydropower and water resource engineering*, Professional Standard of the People's Republic of China, China Electric Power Press, Beijing, China, 2005.

[31] M. Lugeon, *Barrages et Geologic Methods de Recherché Terrasement et un Permeabilization*, Litrairedes Universite, Paris, France, 1933.

[32] ASTM D2166 / D2166M-16, Standard Test Method for Unconfined Compressive Strength of Cohesive Soil, ASTM International, West Conshohocken, PA, 2016.